Materials Innovations

HΣXA Publishers

Research Article | Superconducting Materials | http://doi.org/10.54738/MI.2023.3701

Thermal Fluctuation Induced Excess Conductivity Analysis of Au Nanoparticles and CuTl-1223 Superconducting Phase Composites

M Mumtaz[1]*, Arshid Khan[1], M Rahim[1], Mubasher[2]

1 Department of Physics, Faculty of Sciences (FS), International Islamic University (IIU), 44000, Pakistan
2 Department of Physics, Faculty of Engineering and Sciences (FEAS), Riphah International University, I14, 44000, Islamabad, Pakistan

OPEN ACCESS

Received: 04 April 2023
Accepted: 13 June 2023
Published: 28 July 2023

Citation: Mumtaz M, Khan A, Rahim M, Mubasher (**2023**) Thermal Fluctuation Induced Excess Conductivity Analysis of Au Nanoparticles and CuTl-1223 Superconducting Phase Composites. *Materials Innovations 3* (7), 74-81.

***Correspondence**: (M Mumtaz)
*mmumtaz75@yahoo.com

Published By Hexa Publishers

ISSN
Electronic: 2790-1963

Fluctuation induced conductivity (FIC) analysis of $(Au)_y$/CuTl-1223 (y = 0, 0.5, 1.0 and 1.5 wt. %) nanoparticles-superconductor composites was carried out via Aslamazov-Larkin (AL) and Lawrence-Doniach (LD) models in different fluctuation regions near and above the critical temperature T_c in the transition region. Different superconductivity parameters, like coherence length along c-axis (ξ_c), inter-layer coupling constant (J), phase relaxation time (τ_φ), Fermi velocity (V_F), Fermi energy (E_F), penetration depth ($\lambda_{p.d}$), critical magnetic field (B_c), lower critical magnetic field (B_{c1}), upper critical field B_{c2} and critical current density (J_c) were calculated with the help of FIC analysis. Almost all these superconducting parameters were increased with the increasing concentration of Au nanoparticles in these composites. The enhancement in these parameters can be attributed to the conducting nature of Au nanoparticles (NPs) residing on the grain boundaries of the host CuTl-1223 superconducting matrix. The suppression of some critical parameters like B_c, B_{c1} and J_c with the addition of Au NPs reflected the paramagnetic nature of Au NPs.

Keywords: Gold Nanoparticles, CuTl1223 superconducting phase, Composites, Fluctuation induced conductivity (FIC) analysis

INTRODUCTION

Thermal fluctuations arise in the oxide high temperature superconductors (HTSCs) due to their anisotropic behavior and short coherence length along c-axis (ξ_c)[1–5]. A lot of experimental as well as theoretical work has been reported on critical effects of thermal fluctuations e.g. the fluctuation induced excess conductivity and magnetic conductivity. Thermal fluctuations are of immense interest in studying the phase transition from normal state to superconducting state at the onset temperature T_c^{onset}(K) of the superconductivity. These fluctuations result in the formation of Cooper pairs in the transition region from T_c^{onset}(K) to T_c (0), which becomes the source of excess conductivity in the transition region of HTSCs[6–10]. The FIC analysis of the bulk as well as the thin films samples of different HTSCs have already been reported by many

groups[11–20]. The FIC analysis helps to estimate the different superconducting microscopic critical parameters of superconducting materials that are very diffi cult to measure directly by the experiments[21]. This analysis provides information about the fluctuation in pairing and scattering mechanism near T_c^{onset}(K)[22].

To investigate the effects of these fluctuations on excess conductivity, Aslamazov-Larkin (AL) model, Lawrence-Doniach (LD) model, Maki–Thompson (MT) model and Hikami–Larkin (HL) model. The FIC ($\Delta\sigma$) were used[23–27].

$$\triangle\sigma(T) = \frac{1}{\rho(T)} - \frac{1}{\rho_n(T)} \tag{1}$$

Where ρ(T) is the actual resistivity, ρ_n(T) is the extrapolated normal state resistivity to 0 K following the straight-line equation α is the intercept and β is the slope that is obtained from fitting of the resistivity versus temperature plot.

AL model is used to explain superconducting fluctuations in intra-grain and inter-grain regions of layered superconductors[16]. The analysis of AL model is generally valid for the single crystalline samples but it can be applied to polycrystalline materials with certain limitations[9]. The excess conductivity according to AL model can be written as;

$$\triangle\sigma(T) = A\varepsilon^{\lambda_D} \tag{2}$$

Where A, ε and λ_D are fluctuation amplitude, reduced temperature and critical exponent respectively. The mathematical expressions for A and ε are given by[16];

$$\varepsilon = \frac{T - T_c^{mf}}{T_c^{mf}} \tag{3}$$

$$A = \begin{cases} e^2/(32\hbar\xi_c(0)) \ \ for\ 3D \\ e^2/16\hbar d \ \ for\ 2D \end{cases} \tag{4}$$

Where T_c^{mf} in equation is the mean field critical temperature determined from the peak of dρ/dT plot, $\hbar$ is the reduced Plank's constant and d is the effective interlayer spacing. The critical exponents are determined by the following relation (5)[28–32];

$$\lambda_D = \frac{D}{2} - 2 \tag{5}$$

Where D is the dimensionality of fluctuations i.e. D = 3 for 3 dimensional fluctuations, 2 for 2 dimensional fluctuations and 0 for zero dimensional fluctuations. Values of λ_D are -1/3, -1/2, -1 and -2 for critical, 3D, 2D and 0D fluctuations, respectively. The LD model is used to calculate $\xi_{c(0)}$ for bulk superconductors at cross-over temperature from 3D to 2D regime (T_{3D-2D}), as follows[33].

$$T_{3D-2D} = T_c\left(1 + \left(\frac{2\xi_c(0)}{d}\right)^2\right\} \tag{6}$$

In this equation, $\left(\frac{2\xi_c(0)}{d}\right)^2 = J$, is the interplane coupling constant. The anisotropy parameter 'γ' is defined as, $\gamma = \xi_{ab}/\xi_c$, where ξ_{ab} and ξ_c are the coherence lengths along the superconducting ab-planes and along c-axis, respectively[33]. The values of ξ_{ab} for CuTl-based HTSCs vary between 10 to 20 Å[34].

The excess conductivity according to MT model is caused by the interaction of fluctuating Cooper pairs with normal electrons[23]. Although the MT contribution is minimal but can't be ignored. This model is dependent on the phase relaxation time and can be used to investigate the influence of the superconducting electrons on the normal electrons[24]. The expression for excess conductivity according to MT model is given by[26];

$$\Delta\sigma_{MT} = \left(\frac{e^2}{8\hbar d\varepsilon(1-\alpha/\delta)}\right] \times ln\left(\left(\frac{\delta}{\alpha}\right)\left(\frac{1+\alpha+(1+2\alpha)^{1/2}}{1+\delta+(1+2\delta)^{1/2}}\right\}\right]$$

Where $\delta = \left(\left(\frac{4\xi_c(0)}{d}\right)^2\left(\frac{k_B T\tau_\varphi}{\pi\hbar}\right)\right]$ represents pair breaking parameter, k_B is the Boltzmann constant and τ_φ is phase relaxation time. The MT contribution depends on τ_φ and in 2D fluctuations region, its importance becomes dominant due to moderate breaking of Cooper pairs[30]. The expression for phase relaxation time of fluctuating Cooper pairs can be written as[29]:

$$\tau_\varphi = \frac{\pi\hbar}{8K_B T\varepsilon_o} \tag{8}$$

Where ε_o is the cross over temperature from 2D (LD) to 0D (MT) fluctuations regime at which $\delta \approx \alpha$[35]. The 0D region exists at temperatures much higher than T_c, where the thermal and pairing energy of electrons compete, so the pairs do not have sufficient time to conduct but exist. The importance of this region is that the Cooper pair's formation starts at temperatures much higher than T_c but due to much higher thermal energy available for breaking of the pairs, they can't establish superconductivity[2].

The Fermi velocity (V_F), Fermi energy (E_F) and coupling constant (λ) of cooper pairs can be calculated from the following equations[9,36]:

$$V_F = \frac{5\pi k_B T_c \xi_c(0)}{2K\hbar} \tag{9}$$

Where K is co-efficient of proportionality and its value is K ≅ 0.12[18].

$$\lambda = \frac{\hbar\tau_\varphi^{-1}}{2\pi k_B T} \tag{10}$$

$$E_F = \frac{h}{\tau_\varphi(1.6\times10^{-19})}(eV) \tag{11}$$

At the critical-3D crossover temperature (T_G), we can use Ginsburg–Landau (GL) theory to calculate some important superconductivity parameters[37]. To find the thermodynamic critical magnetic field $B_c(0)$, we use the Ginsburg number N_G, as follows[38,39];

$$N_G = \left(\frac{T_G - T_c}{T_c}\right| = \frac{1}{2}\left(\frac{k_B T_c}{B_{c(0)}^2\gamma^2\xi_{c(0)}^3}\right]^2 \tag{12}$$

$$B_c = \frac{\Phi_o}{2\left(\sqrt{2}\right)\pi\lambda_{p.d}\xi_{ab}(0)} \tag{13}$$

$$B_{c1} = \frac{B_c ln\kappa}{\left(\sqrt{2}\right)\kappa} \quad (14)$$

$$B_{c2} = \left(\sqrt{2}\right)\kappa B_c \quad (15)$$

$$J_c = \frac{4\kappa B_{c1}}{3\sqrt{3}\lambda_{p.d} ln\kappa} \quad (16)$$

Where, $\Phi_o = \frac{h}{2e}$ and $\kappa = \frac{\lambda_{p.d}}{\xi}$ are the flux quantum and GL parameter, respectively[40].

In this article, we have presented the results of the fluctuation induced conductivity analysis of $(Au)_z$/CuTl-1223 nanoparticles-superconductor composites. The objective behind the inclusion of Au NPs in the CuTl-1223 matrix was to fill the voids between the superconducting grains and to enhance the inter-grains connectivity with the conducting natured NPs to improve the superconducting transport properties. In order to further elaborate the experimental study, we have carried out the FIC analysis of the resistivity data. From this analysis it was observed that the Josephson's coupling parameter J and λ were increased with the addition of Au NPs. This shows that the superconductivity is enhanced due to the improved inter-grain coupling caused by the conducting Au NPs added across the grain-boundaries.

EXPERIMENTAL

Au NPs were extracted from gold colloidal solution, while CuTl-1223 superconducting matrix was synthesized via two-step solid-state reaction method. In first step, the calculated amounts of $Ca(NO_3)_2.4H_2O$, $Ba(NO_3)_2$ and $Cu_2(CN)_2.H_2O$ were mixed and ground for about two hours in an agate mortar and pestle. After grinding, the ground material was kept in quartz boat and then placed in a chamber furnace at 860 ^oC for 24 hours and then cooled down the material to room temperature. Further, the material was again ground for an hour and again heat-treated at 860 ^oC for 24 hours in pre-heated chamber furnace. In this way, the precursor $Cu_{0.5}Ba_2Ca_2Cu_3O_{10-}$ material was obtained. In the second step, the calculated amount of Thallium Oxide (Tl_2O_3), Au NPs and precursor material were mixed and ground one hour. The ground material was pressed under a high pressure of 3.8 tons / cm^2 using a hydraulic press to obtain the samples in pellets form. These samples were enclosed in gold capsules for sintering at 860 ^oC for about 10 minutes in pre-heated chamber furnace followed by quenching to room temperature to get $(Au)_z$/CuTl-1223 composites.

The resistivity versus temperature measurements of the samples have been carried out via four probe technique by using Quantum Design Physical Properties Measurement System (PPMS). The FIC analysis of the samples was performed by AL and LD models to deduced different superconducting parameters.

RESULTS & DISCUSSION

The combined graph of resistivity versus temperature of $(Au)_z$/CuTl-1223 composites is shown in Figure 1. In the inset of Figure 1, the variation of T_c and ρ_{300K} versus (vs) Au nanoparticles (z) contents is also given. The values of T_c for $(Au)_z$/CuTl-1223 samples with z = 0, 0.5, 1.0 and 1.5 wt.% was found around 87.28 K, 97.32 K, 101.33 K and 95.31 K, respectively. It was observed that the value of T_c is increased with the addition of Au NPs up to certain optimum level (i.e. z = 1.0 wt.%) and then started to decrease beyond this optimum contents of Au NPs. The initial enhancement of $T_c(0)$ is attributed to the improvement of inter-grains connectivity by healing up the voids and pores present in the host CuTl-1223 matrix with conducting Au NPs, while the decrease in T_c beyond the optimum level may be due to segregation and agglomeration of non-superconducting Au NPs at the grain boundaries of the host CuTl-1223 superconducting matrix. This segregation and agglomeration result into the suppression of superconducting volume fraction and density of charge carriers in the conducting CuO_2 planes of CuTl-1223 superconductor. The resistivity vs temperature measurements show that the normal state resistivity at 300 K (ρ_{300K}) is decreased up to optimum concentration level of Au NPs. The suppression of ρ_{300K} may be due to the suppression of weak-links among the superconducting grains, which may promote the charge carriers transport processes and decrease the energy losses at the grain boundaries. Beyond the optimum level, enhancement in the normal state resistivity may arise due to higher scattering and trapping of charge carriers with agglomerated Au NPs present at the grain boundaries[37,38]. The variation of T_c and ρ_{300K} is somehow random with Au NPs addition. This random behavior may be due to non-uniform distribution of these nanoparticles at the grain-boundaries of the host CuTl-1223 superconductor[41].

The FIC analysis of resistivity versus temperature data of $(Au)_z$/CuTl-1223 composites have been performed via various theoretical models such as AL and LD models along with GL theory in different transition regions. The log-log plots of excess conductivity ($\Delta\sigma$) versus reduced temperature (ε) for $(Au)_z$/CuTl-1223 composites are shown in Fig. 2 (a-d). The combined plot of actual measured resistivity (ρ), extrapolated normal state resistivity (ρ_n) from room temperature to 0 K and $d\rho/dT$ for all samples are given in the insets of Figure 2 (a-d).

The fitting of experimental curves shows the presence of different fluctuation regions such as critical, 3D, 2D and 0D regions in these samples. The numerical values of different superconducting parameters such as $T_c(0)$, T_c^{mf}, all cross over tem-

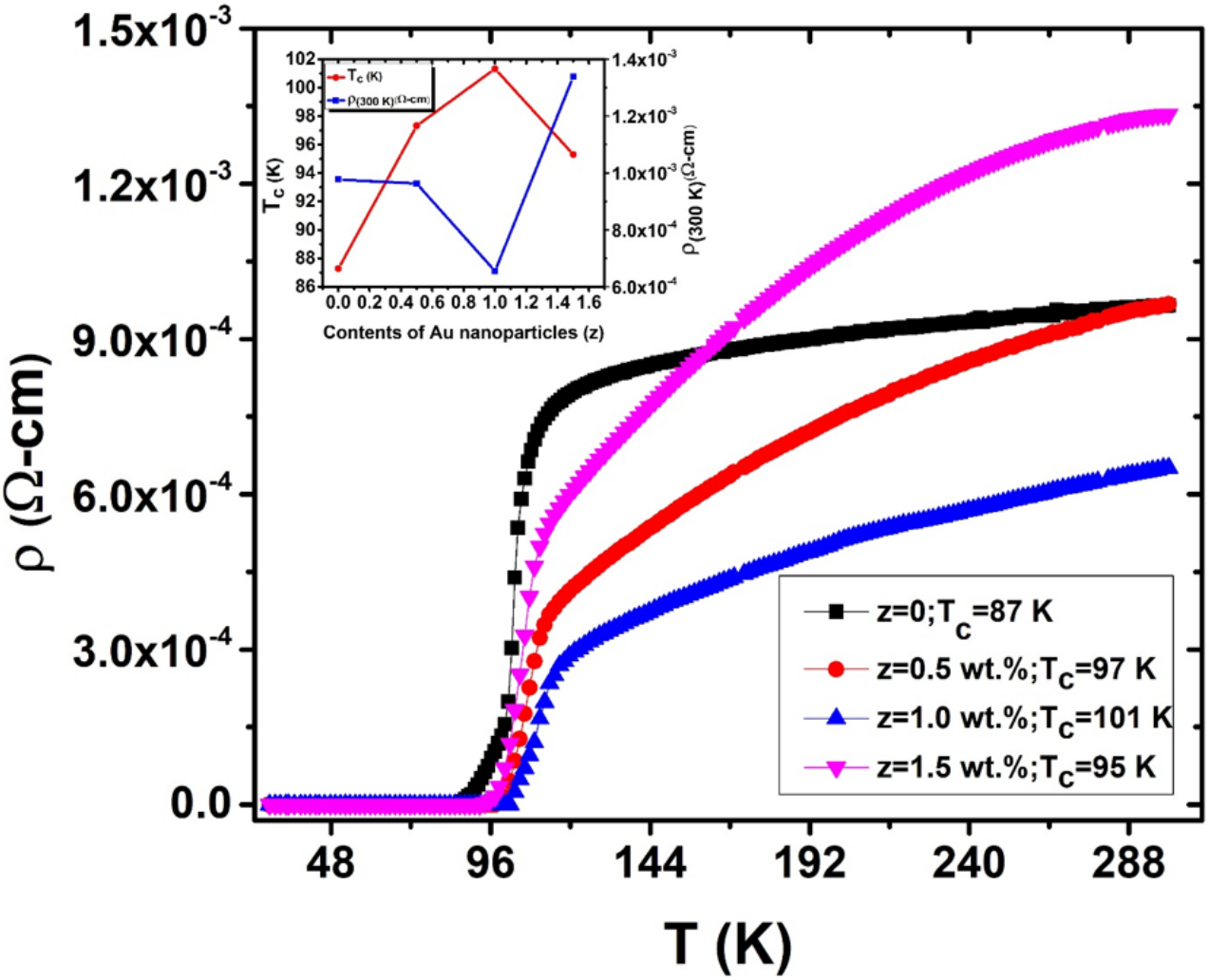

Figure 1. Resistivity versus temperature measurements of $(Au)_z$/CuTl-1223composites.

Table 1. Superconducting parameters extracted from FIC analysis of $(Au)_z$/CuTl-1223 composites.

Sample	Tc (0) (K)	T_c^{mf}(K)	TG(K)	T_{3D-2D} (K)	T_{2D-0D} (K)	T*(K)	$\alpha=\rho_n$ (0K) $(m\Omega-cm)$	ΔT_c (K)	$\xi_c(0)$ (´)	$J=(2\xi c(0))^2/d^2$
z=0.0	87.28	102.34	103.44	104.35	120.40	145.31	0.76	4.30	1.05108	0.01964
z=0.5	97.32	107.35	109.36	120.40	133.44	140.46	0.17	10.25	2.61496	0.12156
z=1.0	101.33	110.36	112.37	114.38	134.45	151.51	0.56	9.31	1.43142	0.03643
z=1.5	95.31	106.35	108.36	119.39	133.44	155.51	5.27	9.81	2.62622	0.12261

Table 2. Numerical values of dimensional exponents (λ_D)in different fluctuation regions for $(Au)_z$/CuTl-1223 composites.

Sample	λ_{cr}	λ_{3D}	λ_{2D}	λ_{0D}
z = 0	-0.31	-0.55	-1.03	-1.86
z =0.5	-0.36	-0.55	-0.98	-1.954
z = 1.0	-0.35	-0.501	-0.96	-1.96
z = 1.5	-0.38	-0.60	-0.98	-1.87

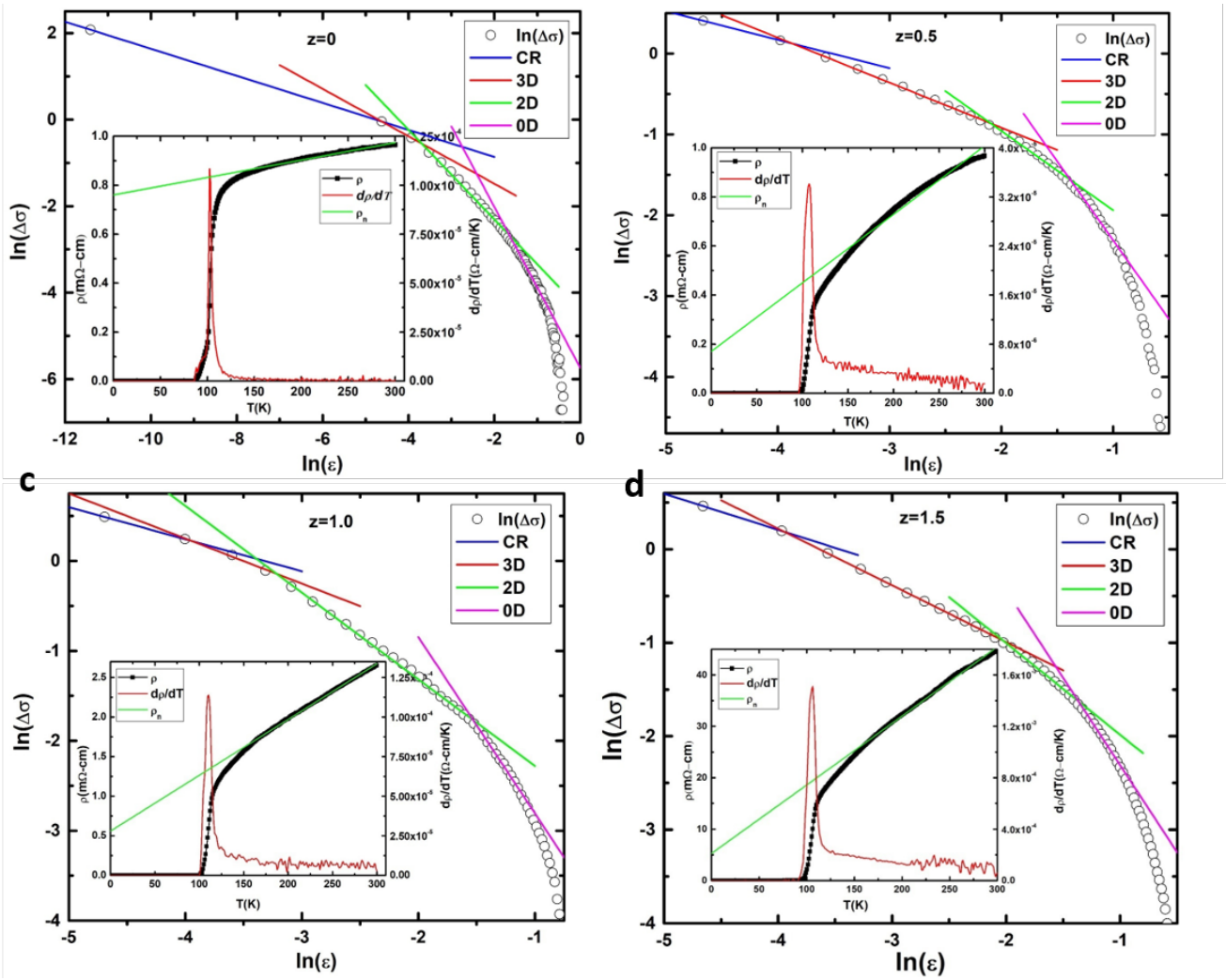

Figure 2. (a) log-log plot of Δσ vs ε for $(Au)_z$/CuTl-1223 composite with z = 0, (b) z = 0.5 wt.%, (c) z = 1.0 wt.%, (d) z = 1.5 wt.%.

Table 3. Temperature ranges of different fluctuationregions for $(Au)_z$/CuTl-1223 composites.

Sample	Critical region(K)	3D region (K)	2D region (K)	0D region (K)
z = 0	102.34 −103.44	103.44– 104.35	104.35– 120.40	120.40 – 152.51
z =0.5	108.36 − 109.36	109.36– 120.40	120.40 –133.44	133.44 – 150.50
z =1.0	111.37 −112.37	112.37 – 114.38	114.38 –134.45	134.45 – 147.49
z =1.5	107.37 −110.38	110.38 – 119.39	119.39 – 133.44	133.44 – 146.48

Table 4. Numerical values of V_F, τφ, λ and E_F of $(Au)_z$/CuTl-1223 composites.

Sample	VF (10^7 cm/s)	(10^{-13} s)	λ	EF (eV)
z = 0	0.786	1.419	0.071	0.175
z =0.5	2.179	0.929	0.098	1.352
z =1.0	1.242	1.028	0.088	0.439
z =1.5	2.144	0.887	0.103	1.308

Table 5. Numerical values of N_G, B_c, $\lambda_{p,d}$, κ, B_{c1}, B_{c2} and J_c of $(Au)_z$/CuTl-1223 composites.

Sample	$N_G \times 10^{-2}$	$B_C(0)$ (T)	$\lambda_{p.d} \times 10^2$ (Å)	κ	B_{C1} (T)	B_{C2} (T)	$J_{C(0)} \times 10^3$ (A/cm^2)
z = 0	1.075	7.172	2.030	13.53	0.976	137.29	19.209
z =0.5	1.872	1.629	8.936	59.58	0.079	137.29	0.991
z =1.0	1.821	4.108	3.545	23.63	0.389	137.29	6.300
z =1.5	1.89	1.608	9.058	60.38	0.077	137.29	0.965

peratures (T_G=T_{CR-3D}, T_{LD}=T_{3D-2D}, T_{MT}=T_{2D-0D}), T^*, α, ΔT_c, $\xi_c(0)$ and J extracted from FIC analysis of resistivity versus temperature data of $(Au)_z$/CuTl-1223 composites are given in Table 1.

It has been observed that the values of T_c (0), T_c^{mf}, T^*, ΔT_c, ξ_c (0), J and all cross over temperatures were increased up to a certain optimum concentration level with the addition of Au NPs. The enhancement in the afore mentioned parameters may arise due to the strong inter-grains coupling caused by addition of conducting Au NPs in the host CuTl-1223 matrix. The value of residual resistivity was decreased with Au NPs addition, which may be due to enhancement of connectivity between the superconducting grains of the host superconducting matrix. The enhanced values of $\xi_c(0)$ show that the samples become more isotropic in nature after addition of Au NPs[40]. The dimensional exponent (λ_D) tells about the dimensionality of superconducting fluctuations. The numerical values of λ_D for different fluctuation regions such as critical, 3D, 2D and 0D regions are listed in Table 2, which have been calculated from the slopes of the lines in different fluctuation regions. The corresponding temperature ranges for λ_D in different fluctuation regions are given in Table 3. It was found that the values of temperature ranges are shifted towards higher values with Au NPs addition as compared to pure sample, which indicates an improvement of the non-superconducting grain boundaries in the host CuTl-1223 superconductor after inclusion of these conducting nanoparticles. The numerical values of V_F, τ_φ, λ and E_F for all samples are listed in Table 4. It has been observed that τ_φ is decreased, while values of V_F, λ and E_F are enhanced, which indicate that the addition of Au NPs promotes the charge carriers transport processes and enhances the coupling between the superconducting grains of host CuTl-1223 matrix. The numerical vales of N_G, B_c, $\lambda_{p.d}$, κ, B_{c1}, B_{c2} and J_c are displayed in Table 5. It can be seen that the values of B_c, B_{c1} and J_c are decreased while the values of N_G, $\lambda_{p.d}$ and κ are increased with the addition of Au NPs. The suppression of critical magnetic fields may be due to paramagnetic behavior of added Au NPs. The value of J_c is also suppressed, which may be due to the increase of the number of mobile carriers scattering sources with the addition of these non-superconducting metallic Au NPs nanoparticles[24].

It has been concluded that most of the superconducting parameters extracted from the FIC analysis have been increased with the addition of Au NPs up to certain optimum level. So it is proposed that the addition of metallic nanoparticles in different granular superconducting matrices is favorable for the improvement of most of the microscopic superconducting parameters.

CONCLUSIONS

Series of $(Au)_z$/CuTl-1223 nanoparticles-superconductor composites were successfully synthesized via solid-state reaction method. The resistivity versus temperature measurements of the samples was carried out via four probe technique and FIC analysis of resistivity vs temperature curves of all these samples was performed by using AL and LD models in different fluctuation regions above T_c. It was found that the values of T_c were increased while ρ(300K) was decreased with Au NPs addition. The enhancement of T_c may be due to improvement of inter-grains connectivity by filling the voids and pores present in the host CuTl-1223 superconductor after inclusion of Au NPs. The values of different superconducting microscopic parameters extracted from FIC analysis such as T_c^{mf}, $\xi_c(0)$, J, V_F, E_F, $\lambda_{p.d}$ and all cross-over temperatures were found to increase with increasing concentration of Au NPs in these composites. The enhancement in these parameters is attributed to the conducting nature of Au NPs residing on the grain-boundaries of the host superconducting matrix. The enhanced values of $\xi_c(0)$ show that the samples become more isotropic as a whole in nature after Au NPs addition. The magnetic properties such as B_c, B_{c1} and J_c were decreased with the addition of Au NPs in CuTl-1223 matrix, which may be attributed to the paramagnetic nature of Au NPs. Most of the superconducting parameters, extracted from FIC analysis were increased with the addition of Au NPs up to certain optimum level.

References

1) Upreti, U. C.; Narlikar, A. V. Excess conductivity, critical region and anisotropy inYBa2Cu4O8. *Solid State Communications* **1996**, *100*, 485–486, available at https://doi.org/10.1016/0038-1098(96.
2) Raza, A.; Rahim, M.; Khan, N. A. Fluctuation induced conductivity analyses of Cd doped Cu0.5Tl0.5Ba2Ca2Cu3−yCdyO10−δ

(y=0, 0.5, 1.0, 1.5) superconductors. *Ceramics International* **2013**, *39* (4), 4349–4354.
3) Al-Sharabi, A.; Abd-Shukor, R. Effect of Re substitution on the formation and fluctuation-induced conductivity of a Tl Sr2(Ca1−Re)Cu2O7−δ (x=0.05−0.30) superconductor. *Ceramics International* **2014**, *40* (7), 9383–9388.
4) Solovjov, A. L.; Dmitriev, V. M. Fluctuation conductivity and pseudogap in YBCO high-temperature superconductors (Review Article)", Low Temp. *Low Temperature Physics* **2009**, *35*, 169–169.
5) Qasim, M. I.; Waqee-Ur-Rehman, M.; Mumtaz, G.; Hussain, K.; Nadeem, K.; Shehzad, Ferromagnetic (Ni) nanoparticles-CuTl-1223 superconductor composites. *The Journal of Magnetism and Magnetic Materials* **2016**, *403*, 60–60.
6) Dadras, S.; Liu, Y.; Chai, Y. S.; Daadmehr, V.; Kim, K. H. Increase of critical current density with doping carbon nano-tubes in YBa2Cu3O7−δ. *Physica C: Superconductivity* **2009**, *469* (1), 55–59.
7) Nakashima, K.; Chikumoto, N.; Ibi, A.; Miyata, S.; Yamada, Y.; Kubo, T.; Suzuki, A.; Terai, T. Effect of ion-irradiation and annealing on superconductive property of PLD prepared YBCO tapes. *Physica C: Superconductivity and its Applications* **2007**, *463-465*, 665–668.
8) Hamrita, A.; Azzouz, F. B.; Dachraoui, W.; Ben salem, M. The Effect of Silver Inclusion on Superconducting Properties of YBa2Cu3O y Prepared Using Planetary Ball Milling. *Journal of Superconductivity and Novel Magnetism* **2013**, *26* (4), 879–884.
9) Mumtaz, M.; Bhatti, A. I.; Nadeem, K.; Khan, N. A.; Saleem, A.; Hussain, S. T. Study of CuO Nano-particles/CuTl-1223 Superconductor Composite. *Journal of Low Temperature Physics* **2013**, *170* (3-4), 185–204.
10) Nawazish, A.; Khan, A.; Saleem, S. Q.; Abbas, M.; Irfan, Ni Nanoparticle-Added Nix/(Cu0.5Tl0.5)Ba2Ca2Cu3O10-δ Superconductor Composites and Their Enhanced Flux Pinning Characteristics. *Journal of Superconductivity and Novel Magnetism* **2018**, *31*, 1013–1013.
11) Nawazish, A.; Khan, Y.; Sekita, H.; Ihara, A.; Maqsood, Growth kinetics of Cu1−xTlxBa2Ca2Cu3O10−y thin films". *Physica C* **2002**, *377*, 43–43.
12) Antipov, E. V.; Abakumov, A. M.; Putilin, S. N. Chemistry and structure of Hg-based superconducting Cu mixed oxides. *Superconductor Science and Technology* **2002**, *15* (7), R31–R49.
13) Tokiwa, K.; Aota, H.; Kunugi, C.; Tanaka, K.; Tanaka, Y.; Iyo, A.; Ihara, H.; Watanabe, T. Pressure effect on Tc in (Cu,Tl)Ba2Ca2Cu3Oy superconductor. *Physica B: Condensed Matter* **2000**, *284-288*, 1077–1078.
14) Tanaka, K.; Iyo, A.; Tanaka, Y.; Tokiwa, K.; Tokumoto, M.; Ariyama, M.; Tsukamoto, T.; Watanabe, T.; Ihara, H. Low superconducting anisotropy (γ=5–11) in (Cu,Tl)-1223 superconductors. *Physica B: Condensed Matter* **2000**, *284-288*, 1081–1082.
15) Tanaka, K.; Iyo, A.; Terada, N.; Tokiwa, K.; Miyashita, S.; Tanaka, Y.; Tsukamoto, T.; Agarwal, S. K.; Watanabe, T.; Ihara, H. Tl valence change and Tc enhancement (>130 K) in (Cu,Tl)Ba2Ca2Cu3Oydue to nitrogen annealing. *Physical Review B* **2001**, *63*, 64508–64508.
16) Mumtaz, M.; Ali, L.; Waqee-Ur-Rehman, M.; Nadeem, K.; Hussain, G.; Abbas, G.; Majeed, B. Improvement in Superconducting Properties of Cu 0.5 Tl 0 . 5 Ba 2 Ca 2 Cu 3 O 1 0 − δ Phase by Addition of γ-Fe 2 O 3 Nanoparticles. *Journal of Superconductivity and Novel Magnetism* **2017**, *30* (10), 2741–2749.
17) Lee, P. A.; Nagaosa, N.; Wen, X.-G. G. Doping a Mott insulator: Physics of high-temperature superconductivity. *Reviews of Modern Physics* **2006**, *78* (1), 17–85.
18) Arif, M.; Rahim, M.; Khan, N. A. Enhanced coherence length and interplane coupling by Ti doping in (Cu, Tl)-1223 superconductors: Para conductivity analyses. *Ceramics International* **2020**, *46*, 3218–3218.
19) Sedky, A.; Youssif, M. I. Structural and Fluctuation Induced Excess Conductivity in R:1113 Superconductors. *Brazilian Journal of Physics* **2016**, *46* (2), 198–205.
20) Muzaffar, M. U.; Safeer, S. H.; Khan, N. A.; Khurram, A. A.; Subhani, T.; Nazir, R. Grain Boundary Shortening in CuTl-1234 Superconductor by the Addition of ZnO Nanoparticles. *Journal of Superconductivity and Novel Magnetism* **2018**, *31* (6), 1669–1675.
21) Ramallo, M. V.; Pomar, A.; Vidal, F. In-plane paraconductivity and fluctuation-induced magnetoconductivity in biperiodic layered superconductors: Application to YBa2Cu3O7-δ". *Physical Review B* **1996**, *54*, 4341–4341.
22) Hannachi, E.; Slimani, Y.; Ekicibil, A.; Manikandan, A.; Azzouz, F. B. Excess conductivity and AC susceptibility studies of Y-123 superconductor added with TiO2 nano-wires. *Materials Chemistry and Physics* **2019**, *235*, 121721–121721.
23) Nayak, P. K.; Ravi, S. Excess conductivity and magneto-conductivity studies of pure and Ag-doped (La1-xYx)2Ba2CaCu5Oz superconductors". *Superconductor Science and Technology* **2006**, *19*, 1209–1209.
24) Annabi, M.; Ghattas, A.; Zouaoui, M.; Azzouz, F. B.; Salem, M. B. Fluctuation conductivity in nano-sized Al2O3 added (Bi,Pb)-2223 superconductors under applied magnetic field. *Journal of Physics: Conference Series* **2009**, *150* (5), 052008–052008.
25) Naqib, S. H.; Cooper, J. R.; Tallon, J. L.; Islam, R. S.; Chakalov, R. A. Doping phase diagram of Y1-xCaxBa2(Cu1-yZny)3O7-δ from transport measurements: Tracking the pseudogap below Tc. *Physical Review B* **2005**, *71*, 54502–54502.
26) Maki, K.; Thompson, R. S. Fluctuation conductivity of high-Tc superconductors. *Physical Review B* **1989**, *39*, 2767–2767.
27) Hikami, S.; Larkin, A. I. Magnetoresistance of high temperature superconductors". *Modern Physics Letters B* **1988**, *2*, 693–693.
28) Solovjov, A. L.; Habermeier, H.-U. U.; Haage, T. Fluctuation conductivity in YBa2Cu3O7−y films with different oxygen content. I. Optimally and lightly doped YBCO films. *Low Temperature Physics* **2002**, *28* (1), 17–24.
29) Solovjov, A.; Dmitriev, V.; Habermeier, H. U.; Trofimov, I. Analysis of fluctuationconductivity of YBa2Cu3O7−δ t-PrBa2Cu3O7−δ superlattices. *Physical Review B* **1997**, *55*, 8551–8551.
30) Solovjov, A. L.; Habermeier, H. U.; Haage, T. Fluctuation conductivity in YBa2Cu3O7−y films with different oxygen content. II. YBCO films with Tc≈80 K. *Low Temperature Physics* **2002**, *28* (2), 99–108.
31) Passos, C. A. C.; Orlando, M. T. D.; Passamai, J. L.; Mello, E. V. L. D.; Correa, H. P. S.; Martinez, L. G. Resistivity study of the pseudogap phase for (Hg,Re)-1223 superconductors. *Physical Review B* **2006**, *74* (9), 94514–94514.
32) Shen, L. J.; Lam, C. C.; Li, J. Q.; Feng, J.; Chen, Y. S.; Shao, H. M. Thermodynamic fluctuation under high pressure in Hg-1223 superconductors. *Superconductor Science and Technology* **1998**, *11* (11), 1277–1282.
33) Nawazish, A.; Khan, N.; Hassan, M.; Irfan, T.; Firdous, Different regions of fluctuation conductivity in Sn-doped Cu0.5Tl0.5Ba2Ca2Cu3−ySnyO10−δ superconductors. *Physica B: Condensed Matter* **2010**, *405*, 1541–1541.
34) Yusuf, A. A.; Yahya, A.; Khan, N. A.; Salleh, F. M.; Marsom, E.; Huda, N. Effect of Ge4+ and Mg2+ doping on superconductivity, fluctuation induced conductivity and interplanarcouplingof TlSr2CaCu2O7−δ superconductors. *Physica C* **2011**, *471* (363).
35) Solovjov, A. L.; Svetlov, V. N.; Stepanov, V. B.; Dmitriev, V. M. Fluctuation conductivity and critical currents in YBCO films. *Low Temperature Physics* **2003**, *29* (12), 973–981.
36) Nawazish, A.; Khan, A. A.; Khurram, U.; Firdous, S.; Ullah, S.; Khan, Excess conductivity ofPb-doped (Cu0.5-xPbxTl0.5)Ba2Ca2Cu3O10-δsuperconductors". *Physica C* **2012**, *474*, 29–29.
37) Qasim, M. I.; Mumtaz, K.; Nadeem, S.; Abbas, Q. Zinc NanoparticlesatIntercrystalliteSitesof(Cu0.5Tl0.5) Ba2Ca3Cu4O12−δ Superconductor. *Journal of Nanomaterials* **2016**, *2016*, 1–6.
38) Jabbar, A.; Qasim, I.; Waqee-Ur-Rehman, M.; Zaman, M.; Nadeem, K.; Mumtaz, M. Structural and Superconducting Properties of (Al2O3) y /CuTl-1223 Composites. *Journal of Electronic Materials*

2015, *44* (1), 110–116.
39) Sarmiento, M. P. R.; Laverde, M. A. U.; López, E. V.; Téllez, D. A. L.; Roa-Rojas, J. Conductivity fluctuation and superconducting parameters of the YBa2Cu3−x(PO4)xO7–δ material. *Physica B: Condensed Matter* **2007**, *398* (2), 360–363.
40) Hussain, G.; Jabbar, A.; Qasim, I.; Mumtaz, M.; Nadeem, K.; Zubair, M.; Abbas, S. Q.; Khurram, A. A. Activation energy and excess conductivity analysis of (Ag)x/CuTl-1223 nano-superconductor composites. *Journal of Applied Physics* **2014**, *116* (10).
41) Jabbar, A.; Qasim, I.; Khan, S. A.; Nadeem, K.; Waqee-Ur-Rehman, M.; Mumtaz, M.; Zeb, F. Highly coercive cobalt ferrite nanoparticles-CuTl-1223 superconductor composites. *Journal of Magnetism and Magnetic Materials* **2015**, *377*, 6–11.